

# A STUDY OF THE EFFECTS OF A CLOSE APPROACH BETWEEN A PLANET AND A PARTICLE

Formiga, J. K. S. (1), Prado, A.F.B.A (2)

(1) *Technology Faculty-FATEC-SJC, São José dos Campos- SP,(55-12)3905-6157,  
jkennety@yahoo.com.br*

(1)(2) *National Institute for Space Research -INPE-DMC, São José dos Campos- SP, (55-12)3208-  
6201, prado@dem.inpe.br*

**Abstract:** *In this paper we study the close approach between a planet and a particle. It is assumed that the dynamical system is given by two main bodies that are in circular orbits around their center of mass and the particle that is moving under the gravitational attraction of the two primaries. This method has been under study for a long time by several authors (Prado, 2001), where the dynamical system given by the “patched-conics” is used and the motion is assumed to be planar. A series of two-body problems is used to generate analytical equations that describe the problem. Two solutions are considered for the swing-by (clock-wise and counter-clock-wise orbit), to take account the possibility that the particles crosses the line Sun-Planet between the primaries. The goal is to study the orbital change (energy, angular momentum, orbital elements) of the particle after some maneuvers with the planet Jupiter and to know those values after the close approach. Finally, numerical simulations are performed here for Sun-Jupiter system.*

**Keywords:** Swing-by, orbital maneuver, astrodynamics

## 1 Introduction

In aerospace engineer, the spacecraft trajectories can be controlled by thrusters and several physical forces. The determination these trajectories in solar systems considering the gravitational effects is performed by several techniques. In this is paper will be used the Swing-By maneuver (gravity-assist) to analyze missions involving celestial bodies and spacecraft (particle) or celestial bodies and a cloud of particles. The maneuver uses a close approach with a celestial body to modify the energy, angular momentum and velocity of the spacecraft with respect to the Sun. The dynamical system given by the “patched-conics” is used and the motion is assumed to be planar. In literature shows several applications of the swing-by technique: the study of the atmospheric effect in swing-by trajectory [2]; classification of trajectories making a swing-by with the Moon [6], the design missions with multiple lunar swing-bys [4]; considering the possibility to apply an impulse during the passage by the periapsis [7]; the study numerical of the swing-by in three dimensions [5]. The study close approach considering a planet and a cloud of particles [8].

It is know that, when in neighborhoods of a planet, a spacecraft in a Sun orbit experiences perturbations which depend on the relative velocity between the spacecraft and the planet and the distance separating the two at point of close approach. If only the gravitational field of the planet affected the motion of the spacecraft, the vehicle would make is approach along a hyperbolic path. In paper [1] show that, in the discussion of planetary approach, solar gravity may be ignored with the assurance that its effect would not modify the results significantly.

In this paper the maneuver is performed around the Sun-Jupiter system where will be studied the motion of the spacecraft near the close encounter with the planet. The spacecraft leaves the point A, passes by the point P (Fig.1) and goes to the point B. Theses points are chosen in a such way that the influence of the Sun at those two points can be neglected and, consequently, the energy can be assumed to remain constant after B and before A. Thus a series of two-body problems is used to generate analytical equations that describe the problem. In particular, the energy and the angular

momentum of the spacecraft before and after close encounter are calculated, to detect the changes in the trajectory during the close approach.

Finally some numerical simulations are performed with several initial conditions. Two solutions are considered for the swing-by: when the maneuver is performed behind the planet (solution 1) and when the maneuver is performed in front the planet (solution 2). The goal is to study the orbital change (energy, angular momentum, orbital elements) of the particle after some maneuvers whit the planet desired and to know those values after the close approach in order to decrease the fuel expense in space missions.

## 2. The swing-by in two dimensions and mathematical model

The baseline of the patched conic approximation is that in any space domain the trajectory of a spacecraft is determined by only on gravitational field, namely that which dominates. The patched conic theory, it is assumed that the dynamical system is given by two main bodies that are in circular orbits around their center of mass and the particle that is moving under the gravitational attraction of the two primaries. So, in this approach, this problem can be studied assuming a system formed by three bodies: the Sun as the main massive primary ( $M_1$ ), a planet as secondary mass ( $M_2$ ), that is orbiting the  $M_1$  body, and a particle with infinitesimal mass ( $M_3$ ) that remains orbiting the primary and makes a close approach with the  $M_2$ . When  $M_3$  into in the influence sphere of  $M_2$ , the orbital motion of the  $M_3$  around of  $M_1$  was being modify. The Figure 1 explains the geometry involved in the close approach. The dynamical system given by the ‘‘patched-conics’’ is used and the motion is assumed to be planar where this method has been under study in [8].

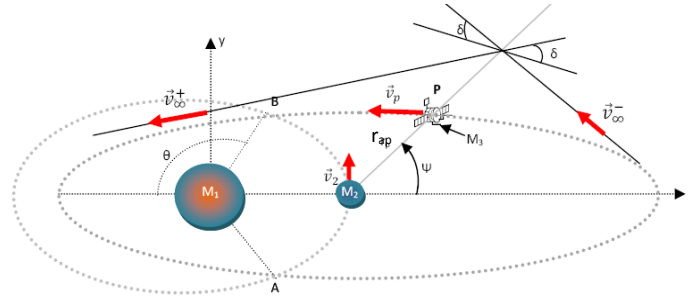


Figure 1. Swing-by variables

In Fig. 1 a set of variables is used here to identify one swing-by trajectory [8]:  $\vec{v}_2$  (velocity of  $M_3$  with respect to  $M_1$ ),  $\vec{v}_{\infty}^-$  and  $\vec{v}_{\infty}^+$  (velocity of  $M_3$  with respect to  $M_2$ , before and after the maneuver in the referential frame),  $\vec{v}_i$  and  $\vec{v}_0$  (velocity of  $M_3$  with respect to  $M_1$ , before and after the maneuver in referential frame),  $\delta$  (half angle curvature),  $r_{ap}$  (the distance from the spacecraft to the center of  $M_2$  at the closest approach moment) and  $\psi$  (angle of approach).

The velocity and orbital elements of the  $M_3$  body are changed when it has a close approach with  $M_2$ . The orbital elements and energy before encounter whit the planet are obtained from the equations:

$$a = \frac{r_a + r_p}{2} \quad (1)$$

$$e = 1 - \frac{r_p}{a} \quad (2)$$

$$E = -\frac{\mu_s}{2a} \quad (3)$$

$$C = \sqrt{\mu_s a (1 - e^2)} \quad (4)$$

which  $a$  = semi-major axis,  $e$  = eccentricity,  $E$ =energy,  $\mu_s=Gm_s=1,33.10^{11}\text{km}^3/\text{s}^2$ .

It is possible to determine the velocity of the particle with respect to the Sun in the moment of the crossing with the planet's orbit and the true anomaly of that point:

$$|v_i| = \sqrt{\mu_s \left( \frac{2}{r_{sp}} - \frac{1}{a} \right)} \quad (5)$$

$$\theta = \cos^{-1} \left[ \frac{1}{e} \left( \frac{a(1-e^2)}{r_{sp}} - 1 \right) \right] \quad (6)$$

The parameter  $r_{sp}$  is distance between the Sun to the planet. The Eq. 6, given us two solutions ( $\theta_A$  and  $\theta_B$ ). The next procedure, it is calculate the angle between the inertial velocity of the particle and the velocity of the planet:

$$\gamma = \tan^{-1} \left[ \left( \frac{e \sin \theta}{1 + e \cos \theta} \right) \right] \quad (7)$$

and the magnitude of particle velocity with respect to the planet in the moment that the approach starts,

$$v_\infty = \sqrt{v_i^2 + v_2^2 - 2v_i v_2 \cos \gamma} \quad (8)$$

This is paper are consider two solutions: assuming a close approach behind the planet (rotation of the velocity vector in counter-clock-wise sense-  $\psi_1$ ) and close approach in front of planet (clock-wise sense-  $\psi_2$ ) for the spacecraft around the Sun (Fig. 2). These two values are obtained from:

$$\begin{aligned} \psi_1 &= 180^\circ + \beta + \delta \\ \psi_2 &= 360^\circ + \beta - \delta \end{aligned} \quad (9)$$

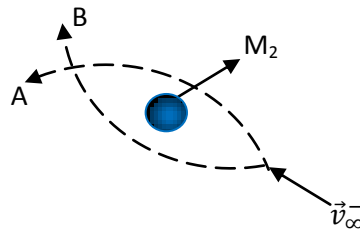


**Figure 2. Possible rotation of the velocity vector**

where

$$\begin{aligned} \beta &= \cos^{-1} \left[ -\frac{v_i^2 - v_2^2 - v_\infty^{-2}}{2 v_2 v_\infty^-} \right] \\ \delta &= \sin^{-1} \left[ \frac{1}{1 + \frac{r_p v_\infty^2}{\mu_p}} \right] \end{aligned} \quad (10)$$

$\mu_p$  is gravitational constant of the planet. The next step is to determine the variations in energy and angular momentum from the equations [3]:

$$\Delta v = \vec{v}_0 - \vec{v}_i = 2|\vec{v}_\infty| \sin \delta \quad (11)$$

$$\Delta E = E_+ - E_- = -\vec{v}_2 \vec{v}_\infty \sin \delta \sin \psi \quad (12)$$

$$\Delta C = \frac{\Delta E}{\omega} \quad (13)$$

Where  $\omega$  is the angular velocity between the primary bodies,  $\delta$  it the angle of deflection and  $E_-$ ,  $E_+$  are the energy before and after maneuver. Through variation in the energy and angular momentum, the orbits are classified in [6]: elliptic direct (negative energy and positive angular momentum), elliptic retrograde (negative energy and angular momentum), hyperbolic direct (positive energy and angular momentum) and hyperbolic retrograde (positive energy and negative angular momentum).

Finally, to obtain the semi-major axis and the eccentricity after the swing-by, it is possible to use the equations

$$a = -\frac{\mu}{2E} \quad (14)$$

$$e = \sqrt{1 - \frac{C^2}{\mu \cdot a}} \quad (15)$$

### 3. Numerical results and simulation procedure

In this study some simulations will be performed to analyze the orbital variation of spacecraft subject a close approach with Jupiter under “patched conics” model, where the physical elements of planets can be seen in Tab 1. The patched conic model was implemented in software Fortran which the energy, angular momentum and orbital elements have been analyzed for several maneuvers. The simulations are completed when the variation energy and angular momentum (Eq. 12) are positive.

**Table 1- Physical elements of Planets**

Planet	Equatorial Radius (km)	Average distance to Sun ( $10^6$ km)	Orbital velocity (km/s)	$\mu=Gm$ ( $10^6$ km <sup>3</sup> /s <sup>2</sup> )
Jupiter	71370	778	13.1	126.0
Saturn	60400	1426	9.7	37.95
$\mu_{sol} = 1.33 \times 10^{11}$ km <sup>3</sup> /s <sup>2</sup>				

All simulations were being performed with following characteristics:

- i) The close approach will be at point A (Fig. 1);
- ii) The Sun does not affect the motion of the particle;
- iii) Will be considered counter-clock-wise orbit and true anomaly  $\theta_A$  (Eq. 6);
- iv) The energy can be assumed to remain constant after B and before A;
- v) The energy and angular momentum will be analyzed after each maneuver for several maneuvers.

- vi) The solution 1 will be performed for the first maneuver behind the planet considering  $\psi_1$  angle of approach and solution 2 for the first maneuver performed in front the planet considering  $\psi_2$  angle of approach.

The initial conditions can be seen in Tab. 2 , where it is composed by:  $r_a$  (apoapsis distance),  $r_p$  (periapsis distance),  $a$  (semi-major axis),  $e$  (eccentricity),  $v$  (velocity),  $E$  (energy) and  $C$  (angular momentum) are obtained from the initial orbit of the spacecraft around the Sun. The  $r_{ap}$  is the distance of the close approach between particle and planet. With the numerical algorithm available, the given initial conditions are changed in any desired range and the number of maneuver and their respective effects of the close approach in the orbit of the spacecraft are studied. The numerical results will be performed in the point A (see Fig. 1) with rotation of the velocity vector in counter-clock-wise sense (solution  $\psi_1$ ) and clock-wise sense (solution  $\psi_2$ ).

### 3.1. Sun-Jupiter System

Three simulations are performed for Sun-Jupiter System where the initial conditions can be seen in Tab. 2. All plots has the first column that was considered the angle of approach  $\psi_1$  (solution 1) and second column that was considered the angle of approach  $\psi_2$  (solution 2).

**Table 2- Initial conditions: Sun-Jupiter System**

Simulations	$r_a$ ( $10^8$ km)	$r_p$ ( $10^8$ km)	$r_{ap}$ (Jupiter's radius)	$a$ ( $10^8$ km)	$e$	$E$ ( $\text{km}^2/\text{s}^2$ )	$C$ ( $10^9$ - $\text{km}^2/\text{s}$ )	$v$ (km/s)
1 <sup>a</sup>	10	3.5	1.5	6.75	0.4814	-98.51	8.3	12.03
2 <sup>a</sup>	10	3.5	30.0	6.75	0.4814	-98.51	8.3	12.03
3 <sup>a</sup>	10	6.5	1.5	8.25	0.2121	-80.61	10.2	13.44

The Fig. 3 show the number of the maneuvers for periapsis distance ( $r_p$ ) considering  $r_a = 10^9$  km and the angle of approach ( $\psi_1$ ) in elliptic orbit around the Sun. This distance has an effect in the results obtained by maneuvers where some simulations were performed to study this problem. Those results allow to analyze the increased in the number of maneuvers for range  $3 \cdot 10^9 \text{ km} \leq r_p \leq 7 \cdot 10^9 \text{ km}$ . This is range implies in regions with  $0.1764 \leq e \leq 0.5385$  and  $6.5 \times 10^8 \text{ km} \leq a \leq 85 \times 10^8 \text{ km}$ . It is possible because increasing the semi-major axis also increase the magnitude of velocity of the particle with respect to the Sun. This change also increase the magnitude of the velocity of the particle with respect to the Jupiter. Thus with Eq.12 is possible to calculate energy variation. This information is essential to analyze the orbital characteristics of the particle before swing-by and the strong influence of  $r_p$  in each mission. Some of these characteristics will be studied with detail in this paper.

In the Fig. 4, the maneuvers performed for  $1 < r_p < 4$  can be analyzed with more details.

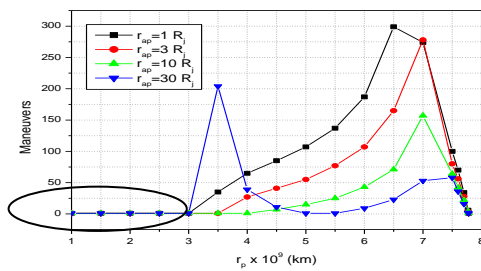


**Figure 3. Maneuvers performed for periapsis distance ( $r_p$ ),  $r_a = 10^9$  km and angle approach ( $\psi_1$ ) in elliptic orbit around the Sun.**

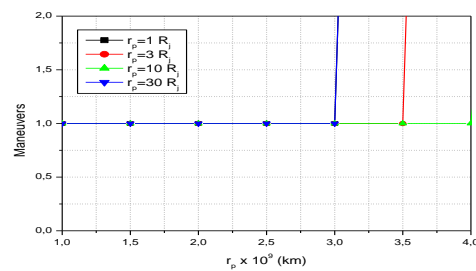
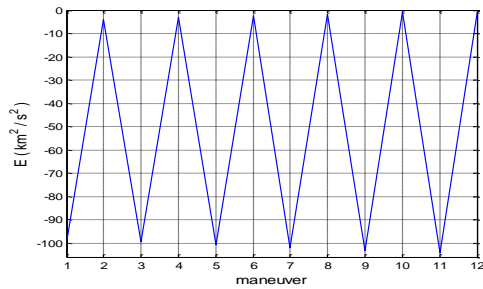
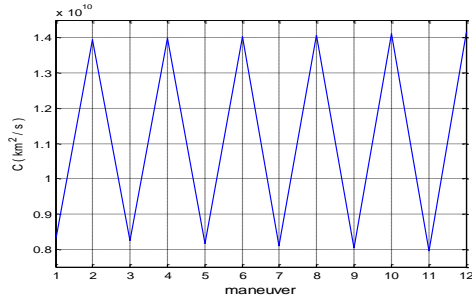


**Figure 4. Zoom of Figure 1 for  $1 < r_p < 4$**

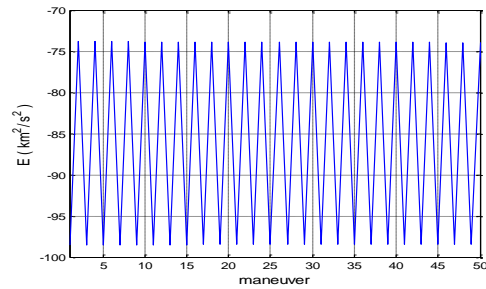
Figures 5 and 6 shows the evolution of the amplitude of energy, angular momentum, semi-major axis, eccentricity and velocity. The results shows two characteristics: maneuver performed behind Jupiter (solution 1) and maneuver performed in front of Jupiter (solution 2). The energy variation for these solutions is enough to increase the orbital elements of the particle where the orbital motion around the Sun is modify. The moment that the particle escapes of orbit can be easily seen from in Fig. 6, in the plot of semi-major axis. The change of energy and angular momentum causes the existence of hyperbolic orbits ( $\Delta E > 0$  and  $\Delta C > 0$ ) and semi-major axis variation leads to eccentricity reaches a maximum value.



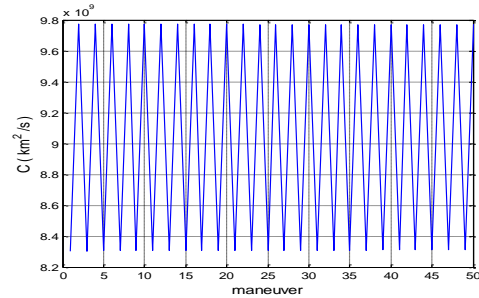
Energy vs maneuver for  $\psi_1$ .



Angular momentum vs maneuver for  $\psi_1$ .

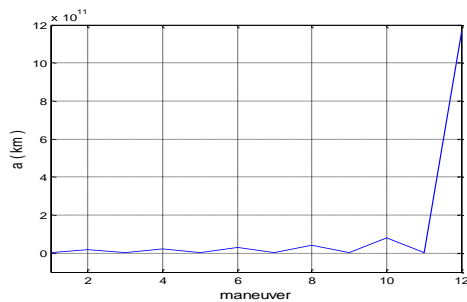


Energy vs maneuver for  $\psi_2$ .

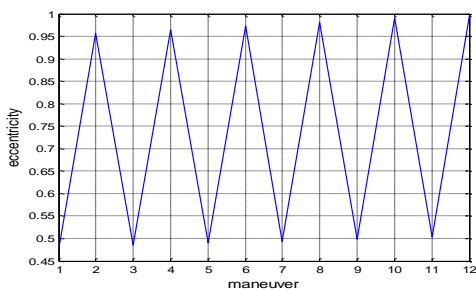


Angular momentum vs maneuver for  $\psi_2$ .

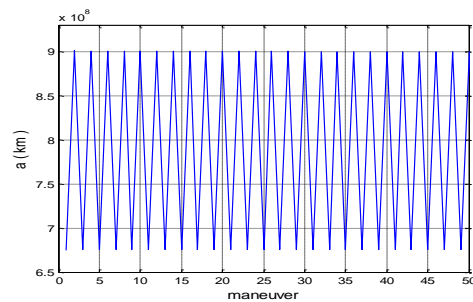
**Figure 5. Energy and angular momentum of the spacecraft after the swing-bys for  $r_a = 10^9$  km,  $r_p = 3.5 \times 10^8$  km,  $r_{ap} = 1.5 R_j$ , considering solution 1 ( $\psi_1$ ) and solution 2 ( $\psi_2$ ).**



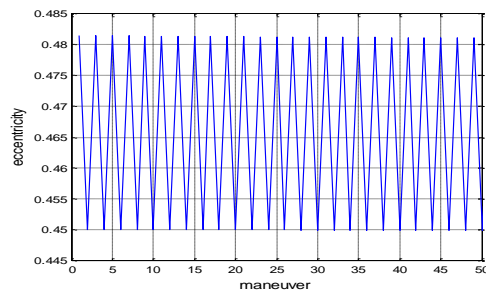
Semi-major axis vs maneuver for  $\psi_1$ .



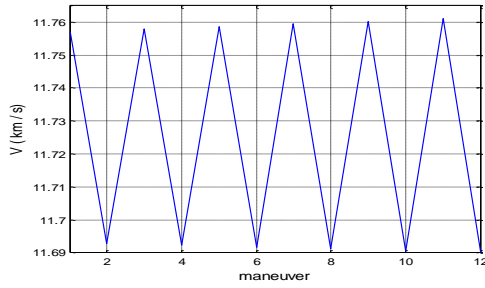
Eccentricity vs maneuver for  $\psi_1$ .



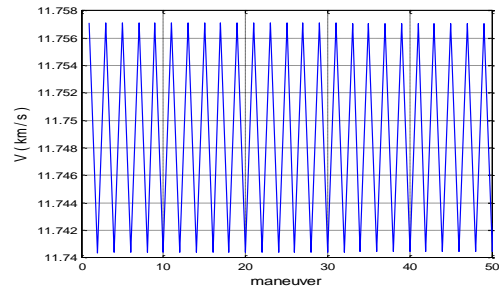
Semi-major axis vs maneuver for  $\psi_2$ .



Eccentricity vs maneuver for  $\psi_2$ .



Velocity vs maneuver for  $\psi_1$ .



Velocity vs maneuver for  $\psi_2$ .

**Figure 6. Semi-major axis, eccentricity and velocity of the spacecraft after the swing-bys for  $r_a = 10^9$  km,  $r_p = 3.5 \times 10^8$  km,  $r_{ap} = 1.5 R_j$ , considering solution 1 ( $\psi_1$ ) and solution 2 ( $\psi_2$ ).**

In Fig. 7 we can see two regions where occurs several maneuvers due to the energy gain and energy loss. In neighborhoods  $-100 \text{ km}^2/\text{s}^2$  (for angle  $\psi_1$ ) and  $-97.5 \text{ km}^2/\text{s}^2$  (for angle  $\psi_2$ ) happen maneuvers with energy loss. Already in neighborhoods  $-2 \text{ km}^2/\text{s}^2$  ( $\psi_1$ ) and  $-75 \text{ km}^2/\text{s}^2$  ( $\psi_2$ ) happen maneuvers with energy gain. For those cases when the  $\psi_1$  (angle of approach) is around 405 degree (45 degree) causes the existence of parabolic orbit because angular momentum is positive and eccentricity equal to 1.0.

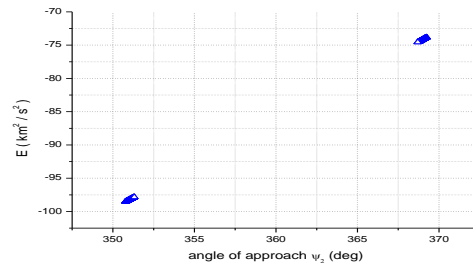
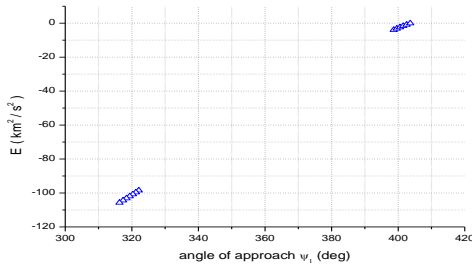
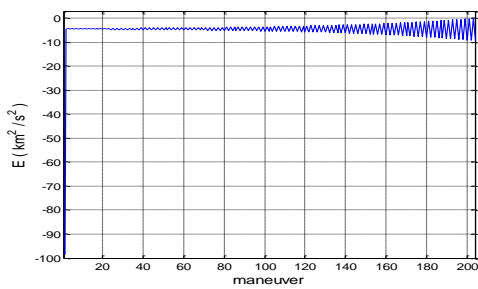
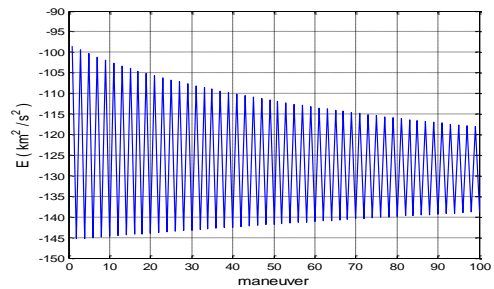


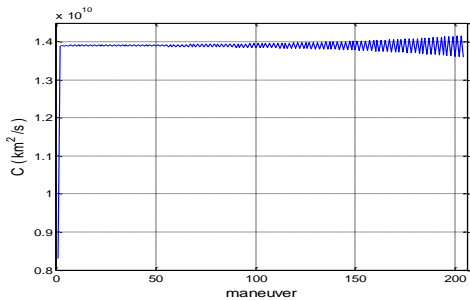
**Figure 7. Energy variation due to the angle of approach of the spacecraft orbits after several swing-bys for  $r_a=10^9$  km,  $r_p=3.5 \times 10^8$  km,  $r_{ap}=1.5 R_j$ .**



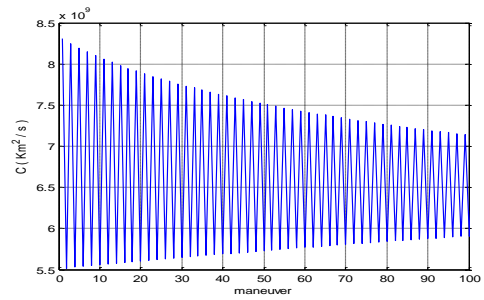
Energy vs maneuver for  $\psi_1$ .



Energy vs maneuver for  $\psi_2$ .



Angular momentum VS maneuver for  $\psi_1$ .



Angular momentum VS maneuver for  $\psi_2$ .

**Figure 8 –Energy and angular momentum of the spacecraft orbits after the swing-bys for  $r_a=10^9$  km,  $r_p=3.5 \times 10^8$  km,  $r_{ap} = 30 R_j$ , considering solution 1 ( $\psi_1$ ) and solution 2 ( $\psi_2$ ).**

The second simulation was performed considering the distance of close approach,  $r_{ap} = 30 R_j$  (radius of Jupiter). These results can be seen in Fig. 8 and Fig. 9 where they show that there are a strong dependence with  $r_{ap}$  and initial conditions. In Fig. 8 for solution 1 is visible the fast orbital change after the first swing-by maneuver. This large change can be seen in all plots for solution 1 (Fig. 9). In general, most of the cases, it is indicates a passage behind the Jupiter that increases the energy of spacecraft. In this case we can see that spacecraft was maneuvered to orbit with high eccentricity (approximately  $e = 1$ ) with  $\Delta E > 0$  and  $\Delta C > 0$ . Another property shown by this figure is that the velocity has small change compared with energy variation where this new configuration of orbit allows up to 200 maneuvers.

Already the solution 2 (Fig. 8 and Fig. 9), where the first maneuver occur in front of Jupiter; we can see the energy loss. When the close approach occur in behind of Jupiter, it acquire energy but  $\Delta E$  decrease at the long time. It is expected because for solution 2, the angle of approach ( $\psi_2$ ) decreases after swing-by maneuver, consequently occur a decrease in energy. This study is made to show the evolution of the amplitudes and the strong influence with the angle of approach where the fuel consumption decreases with this variable. Similar results can be seen in Fig. 10 with respect to the angle of approach.

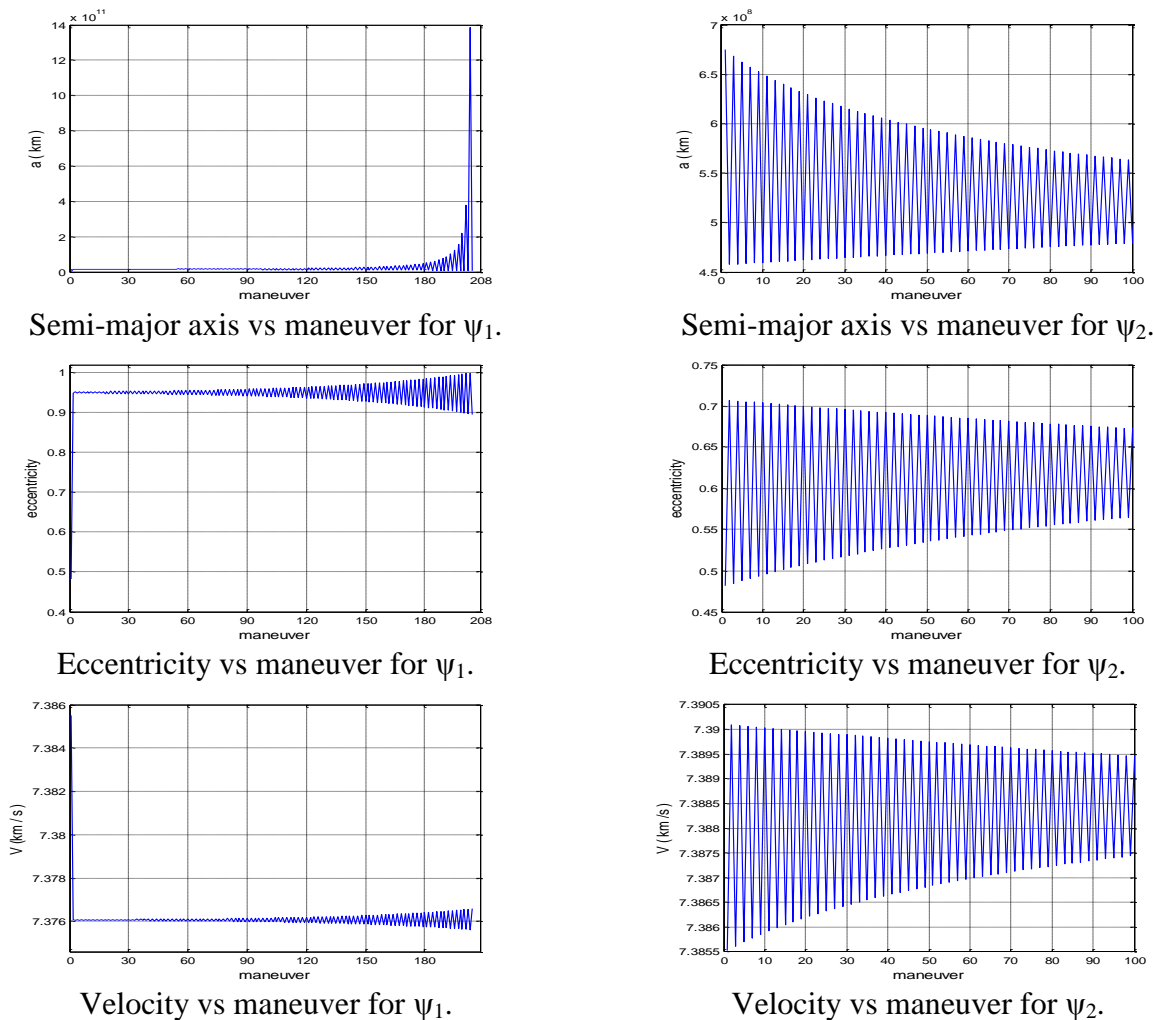


**Figure 9 – Semi-major axis, eccentricity and velocity of the spacecraft after the swing-bys for  $r_a=10^9$  km,  $r_p=3.5 \times 10^8$  km,  $r_{ap}=30 R_j$ , considering solution 1( $\psi_1$ ) and solution 2 ( $\psi_2$ ).**

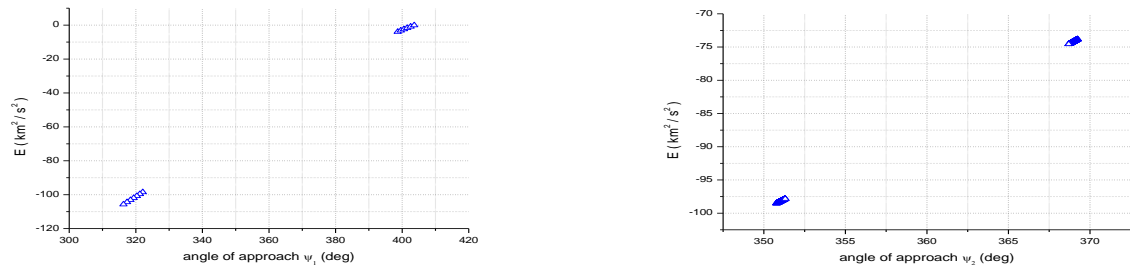


**Figure 10- Energy variation due to the angle of approach of the spacecraft orbits after several swing-bys for  $r_a=10^9$  km,  $r_p=3.5 \times 10^8$  km,  $r_{ap}=30$  Rj, considering solution 1 ( $\psi_1$ ) and solution 2 ( $\psi_2$ ).**

From analyzes of the Fig. 11 and Fig. 12, we can see a difference in the behavior between both solutions. The results show a small influence on the velocity amplitude and that the angle of approach has a strong influence in the energy gain. For solution 1, in most of the cases the amplitude of the energy and orbital elements has a small increase with the maneuvers. This effect can be easily seen in the Fig. 13 due at the angle of approach variation. For all results in solution 2 the amplitudes remained approximately constant which this keeps the spacecraft in elliptic orbit after the swing-by maneuver. We can to conclude that a large modify in orbital characteristic occur due change of  $r_{ap}$ .

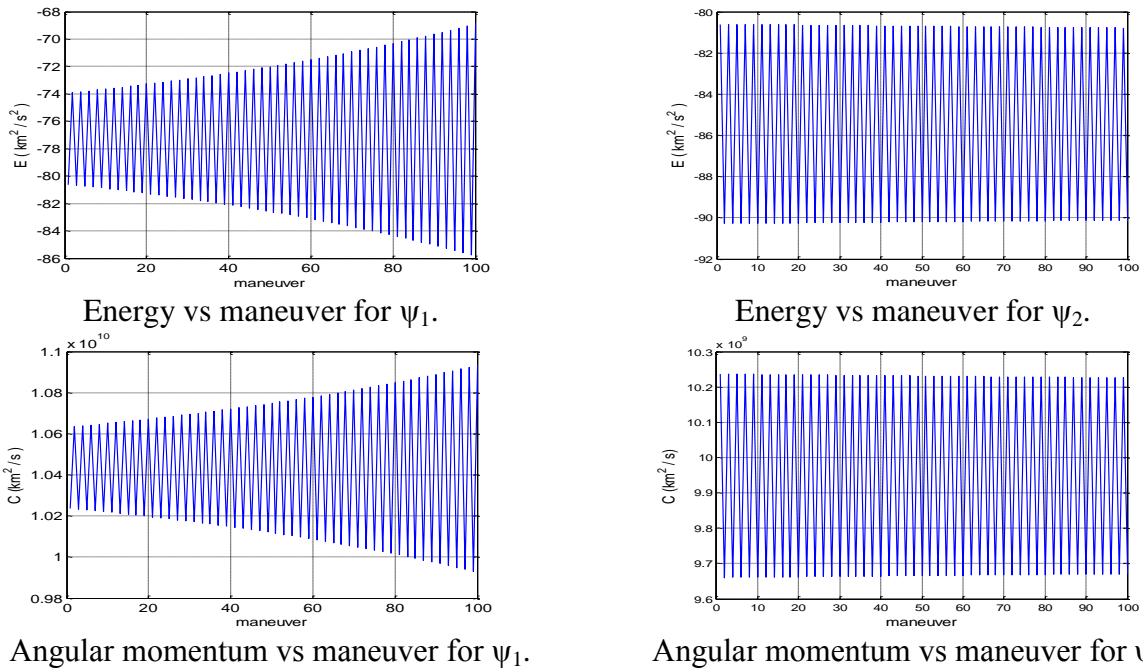
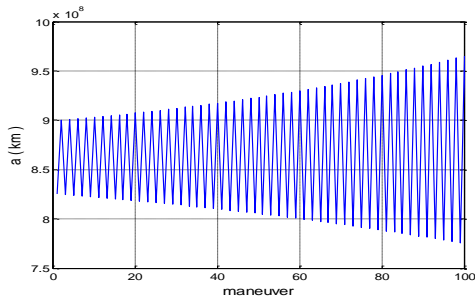
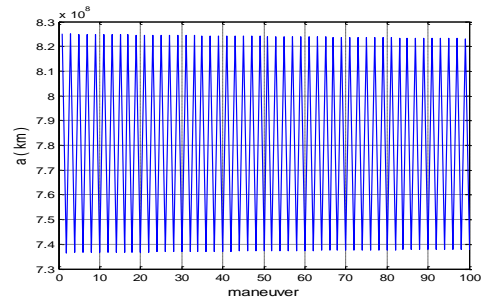


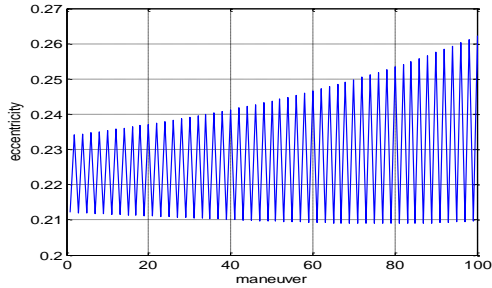
**Figure 11 –Energy and angular momentum of the spacecraft after the swing-bys for  $r_a=10^9$  km,  $r_p=6.5 \times 10^8$  km,  $r_{ap} = 1.5$  Rj, considering solution 1( $\psi_1$ ) and solution 2( $\psi_2$ ).**



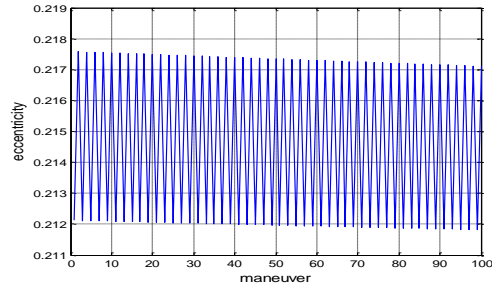
Semi-major axis vs maneuver for  $\psi_1$ .



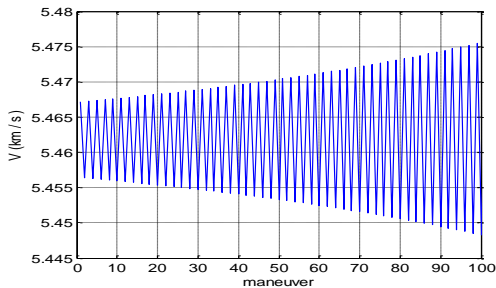
Semi-major axis vs maneuver for  $\psi_2$ .



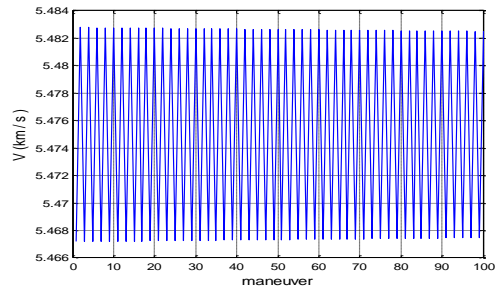
Eccentricity vs maneuver for  $\psi_1$ .



Eccentricity vs maneuver for  $\psi_2$ .



Velocity vs maneuver for  $\psi_1$ .



Velocity vs maneuver for  $\psi_2$ .

**Figure 12 – Semi-major axis, eccentricity and velocity of the spacecraft after the swing-bys for  $r_a=10^9$  km,  $r_p=6.5 \times 10^8$  km,  $r_{ap}=1.5 R_j$ , considering solution 1 ( $\psi_1$ ) and solution 2 ( $\psi_2$ ).**

The Fig. 13 has possible two regions: energy loss around the  $-90 \text{ km}^2/\text{s}^2$  (353 degree) and energy gain around  $-81 \text{ km}^2/\text{s}^2$  (6 degree) for the angle of approach  $\psi_2$ . Already considering the  $\psi_1$  angle of approach we can see the energy variation.

Based in Fig. 14, we can have an overview to analyze the orbital variation for all simulations in Sun-Jupiter system. The simulation 3 has a large difference between the two solutions. It is possible due to the energy gain after swing-by maneuver for solution 1. All the results for solution 2, the orbital characteristic seen in Fig. 13 shows a small variation in orbital elements. These results are critical to determine the appropriate maneuver or to determine energy necessary for maneuvers more economical.

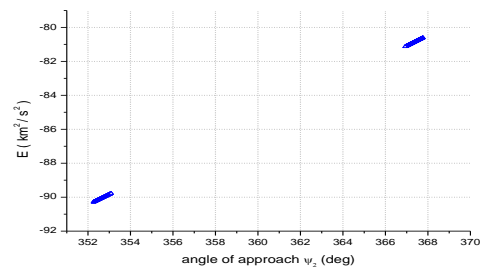
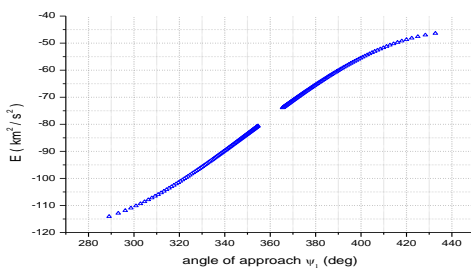
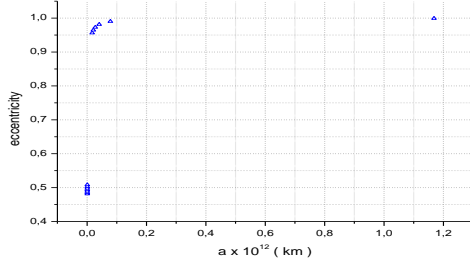
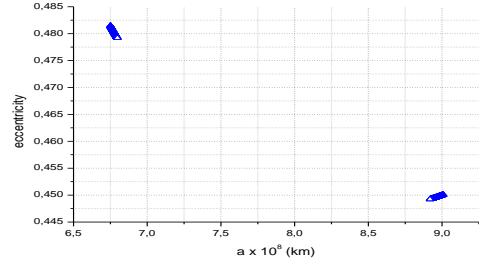


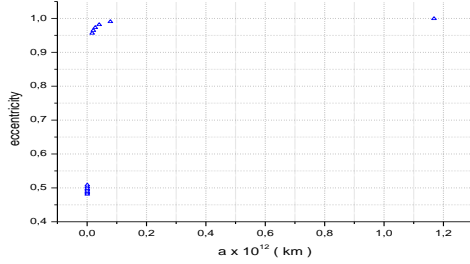
**Figure 13- Energy variation due to the angle of approach of the spacecraft orbits after several swing-bys for  $r_a=10^9$  km,  $r_p=6.5 \times 10^8$  km,  $r_{ap}=1.5 R_j$ , considering solution 1 ( $\psi_1$ ) and solution 2 ( $\psi_2$ ).**



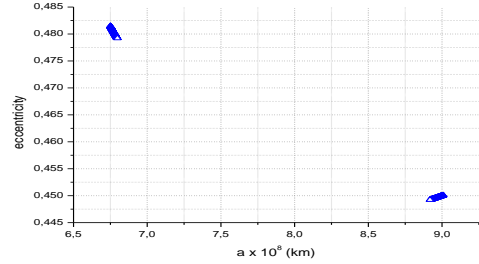
Simulation 1 for solution 1 ( $\psi_1$ )



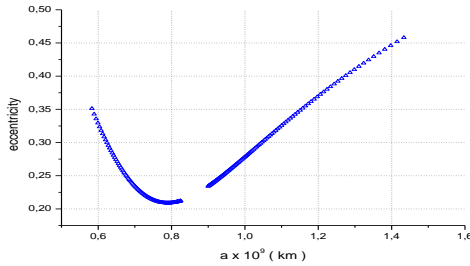
Simulation 1 for solution 2 ( $\psi_2$ )



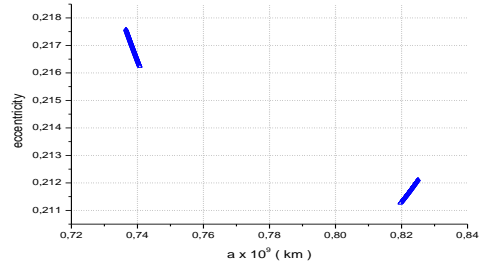
Simulation 2 for solution 1 ( $\psi_1$ )



Simulation 2 for solution 2 ( $\psi_2$ )



Simulation 3 for solution 1 ( $\psi_1$ )



Simulation 3 for solution 2 ( $\psi_2$ )

**Figure 14- Eccentricity VS Semi-major axis for solution 1( $\psi_1$ ) and solution 2( $\psi_2$ ).**

The magnitude of semi-major axis, eccentricity and energy are showed in Tab. 3. It is possible to analyze in more detail the maximum value of amplitude in the orbital characteristic of spacecraft after swing-by maneuver. The Tab. 3 show a great variation for all simulations performed considering the  $\psi_1$  and  $\psi_2$  angle of approach. Based in the initial condition (Tab. 2) we can see that  $\Delta v$  has a minimum value of variation for all simulations performed.

**Table 3-The maximum value of amplitude: energy, momentum, semi-major axis, eccentricity and velocity after the maneuver (Sun-Jupiter System)**

Maximum variation after the maneuver					
Solution 1 ( $\psi_1$ )					
simulation	$\Delta a$ ( $10^8$ km)	$\Delta e$	$\Delta E$ ( $\text{km}^2/\text{s}^2$ )	$\Delta C$ ( $10^9$ - $\text{km}^2/\text{s}$ )	$\Delta v$ (km/s)
<b>1<sup>a</sup></b>	5,25	0,5186	102	0,57	0,07
<b>2<sup>a</sup></b>	7,7	0,4686	93,51	0,55	0,01
<b>3<sup>a</sup></b>	1,9	0,0520	17	0,11	0,027
Solution 2 ( $\psi_2$ )					
<b>1<sup>a</sup></b>	2,7	0,0314	21	0,15	0,020
<b>2<sup>a</sup></b>	1,75	0,2286	46,49	0,01	0,006
<b>3<sup>a</sup></b>	0,9	0,0050	9,84	0,60	0,016

#### 4. Conclusions

This study is made to show the evolution of the amplitudes, the strong influence with the angle of approach and of choice of periapsis position. A method to calculate the variations in semi-major axis, velocity, energy and angular momentum for the Swing-By is developed based in the "patched-conic" approximation. Three numerical simulations are calculated for the Sun-Jupiter system considering several initial conditions. A set of analytical equations is used to describe the swing-by in two dimensions and to evaluate the variation in the orbital elements of the orbit of a spacecraft that is passing by the planet. Then, it is possible to compare analytically two solutions to make an orbital maneuver considering two angle approach  $\psi_1$  and  $\psi_2$ . The results showed that the maneuvers performed for  $\psi_1$  have a great energy gain and in most of the cases the spacecraft escapes. For maneuvers performed for solution 2 where the first close approach happens in front the planet, the spacecraft remains indefinitely for a long time in elliptic orbit due energy loss. The choices of periapsis show a strong influence in the maneuver that can be chosen to obtain low fuel consumption. In Sun-Jupiter system the cases where the spacecraft has escaped the results shown that the vector velocity was doubled compared to initial velocity and the variation of  $\psi$  leads to great energy variation.

#### Acknowledgment

The authors wish to express their appreciation for the support provided by CAPES.

#### References

- [1] Battin, Richard H. An introduction to the mathematics and models of astrodynamics, American Institute of Aeronautics and Astronautics, New York, New York, 1987.
- [2] Broucke, R.A. & A.F.B.A. Prado (1993). "Jupiter Swing-By Trajectories Passing Near the Earth", *Advances in the Astronautical Sciences*, Vol. 82, No 2, pp. 1159-1176.
- [3] Broucke, R. A.(1988) The Celestial mechanics of gravity assist, In:AIAA/AAS Astrodynamics Conference, Minneapolis, MN, August. (AIAA paper 88-4220).
- [4] Dunham, D. & S. Davis (1985). "Optimization of a Multiple Lunar- Swing by Trajectory Sequence," *Journal of Astronautical Sciences*, Vol. 33, No. 3, pp. 275-288.
- [5] Felipe, G. & A.F.B.A. Prado (1999). "Classification of Out of Plane Swing-by Trajectories". *Journal of Guidance, Control and Dynamics*, Vol. 22, No. 5, pp. 643-649.
- [6] Prado, A.F.B.A. & R.A. Broucke (1995). "A Classification of Swing-By Trajectories using The Moon". *Applied Mechanics Reviews*, Vol. 48, No. 11, Part 2, November, pp. 138-142.
- [7] Prado, A. F. B. A., Broucke, R. A. (1996). Transfer orbits in the Earth-Moon system using a regularized model. *Journal of Guidance, Control and Dynamics*, v. 19, n.4, p.929-933.
- [8] Prado, A. F. B. A. (2001) Trajetórias espaciais e a manobras assistidas por gravidade, São José dos Campos-SP, Cruzeiro.